ELETROCHEMICAL REDUCTION OF TITANIUM DIOXIDE 3-D PERIODIC STRUCTURES

By

JEONGWOOK SEO

Master of Science in Chemical Engineering

ChungBuk National University

Cheongju, S.Korea

2004

Submitted to the Faculty

of the Graduate College of the

Oklahoma State University

In partial fulfillment of

the requirements for the Degree of

MASTER OF SCIENCE

December, 2010

ELETROCHEMICAL REDUCTION OF TITANIUM

DIOXIDE 3-D PERIODIC STRUCTURES

Thesis Approved:

Dr. Jim Smay

Thesis Adviser

Dr. AJ Johannes

Dr. Josh Ramsey

Dr. Mark E. Payton

Dean of the Graduate College

ACKNOWLEDGMENTS

First and foremost, I sincerely appreciate my parents for all the care and love that I have received from them all my life. Once more I deeply thank my parent to supporting my M.S study and I would like to thank my sisters who give encouragement to my journey of intellectual pursuit in Oklahoma State University, at school of chemical engineering. Second, I am grateful to my advisor, Dr. Jim Smay, for his guidance and support during my study at OSU. I also appreciate my committees, Dr. AJ Johannes and Dr. Josh Ramsey, for their help. I feel gratitude to Dr. Khaled Gasem to give me a lot of advice to finish my M.S study. For this research, I thank Dr. Jian Xu and Dr. Cheng Zhu gave me the technical support to operate robocasting and rheology measurement. I also thank my friend Andy and Travis Bush for giving me a lot of help my thesis writing. I would like to express my appreciation to all the professors at the School of Chemical Engineering in OSU. I learned a lot from all my class works. I thank all department staff members, Eileen, Carolyn, Shelley, and Mindy for all the help and assistance. Finally, I would like to thank all department graduate students. I have had such a great time in OSU.

This research is based upon work supported by the National Science Foundation for funding this work as part of A CAREER grant, award number DMI-0448702.

TABLE OF CONTENTS

LIST OF TABLES

LIST OF FIGURE

NOMENCLATURE

P_y	Compressive yield stress
Y	Elastic properties of the material
$\emptyset$	Volume fraction of the solid
$\emptyset_{gel}$	Minimum solids loading
K	System specific free-factor
X	Scaling exponent
ΔG	Gibbs free energy
V	Volt
mV	Millivolt
A	Ampere
T	Time
E_{cell}	Cell potential at non standard state conditions
E^{o}_{cell}	Cell potential at standard state conditions
R	Gas constant (J/mole K)
T	Temperature (K)
F	Faraday's constant (C/mole e^-)
C	Coulomb (A/s)

N	Number of electron moles that transferred in the designed reaction mechanism
$\dot{\gamma}$	Shear rate
η_{app}	Apparent viscosity
τ	Shear stress

CHAPTER 1 INTRODUCTION

1.1 Robocasting

There exist numerous solid-freeform fabrication processes to assemble three-dimensional (3-D) freeform structures based on material deposition guided by a computer model. The typical process begins with printing sequential, two-dimensional (2-D) layers by methods such as ink jet printing, [1] 3-D printing, [2-5] and extrusion based deposition[6,7] until the 3-D object is assembled. The extruder printing method can use various materials such as metals, ceramics, and polymers. In this research, a 3-D lattice structure was fabricated by an extrusion-based technique called robocasting.

In the robocasting method, a colloidal gel-based ink is filled into a syringe and extruded through a cylindrical nozzle at a controlled rate. The filament is used to fabricate 3-D structures [8,9] as it is deposited in a controlled 2-D pattern on a flat substrate. After depositon of a layer, the nozzle incrementally increases in height above the printed layer and deposits another pattern atop of the first. This sequence is repeated until the 3-D structure is completed. The robocasting method can use various materials such as ceramics, [10-15] metals, [16] and polymers[17] with the stipulation that the material must be formulated as a colloidal paste for extrusion. Various application studies using this method and materials have been reported as sensors, [11] photonic materials, [12] tissue engineering schaffolds, [14] and composites.[16]

Figure 1.1 shows a computer rendering image of the robocasting hardware used in this study.[13] The syringe is attached to the vertical axis of the robot and moves in X and Y directions to make 2-D patterns and regularly moves in the Z-direction after each layer patterning is finished. A syringe pump controls the extrusion rate. Typical nozzle diameter is in the range of 0.05 to 1mm.

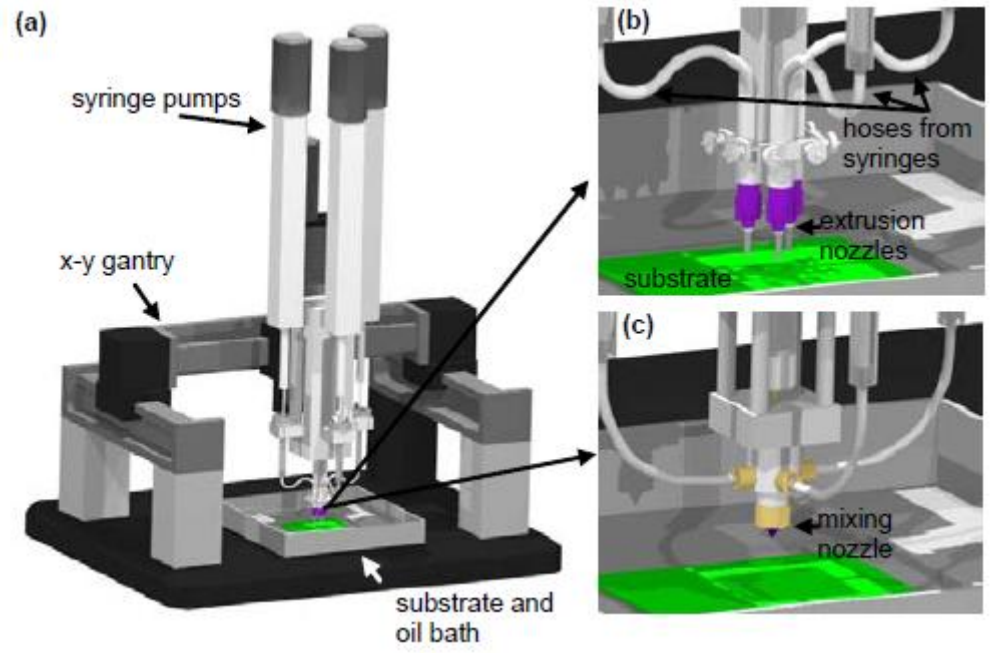

Figure 1.1 (a) Schematic rendering of a gantry robot with three syringe pumps attached, (b) three nozzle deposition heads for discrete printing of various compositions, and (c) mixing nozzle capable of blending three inks. [13]

There are several critical requirements to fabricate structures by robocasting. First, the colloidal ink must be formulated with appropriate flow behavior such that it can flow from the syringe through the nozzle and maintain a cylindrical shape after extrusion. Second, the cylindrical filament must be supple enough to be patterned in a two-dimensional set of lines and promote adherence between layers. Finally, the high solids

volume fraction of the colloidal paste helps the structure dry without warping or cracking. This is followed by a high temperature sintering operation.

The equilibrium elastic properties of the colloidal paste depend on particle concentration and interparticle potentials. The equation for the behavior of colloidal paste elastic properties is shown as the following:[18]

$$y = k\left(\frac{\phi}{\phi_{gel}} - 1\right)^{x} \tag{1.1}$$

Where ϕ is the volume fraction of the solid, ϕ_{gel} is a minimum solids loading for gelation to occur, k is a system specific factor, x is a scaling exponent, and y is the property of interest.

The state of dispersion of the colloidal particles is critical to formulating inks with appropriate flow behavior for the robocasting process. If polyelectrolyte (e.g Polyacrylic acid (PAA) or Polyethylenimine (PEI)) coat the surface of the colloidal particles, the surfaces have same electric charge and a repulsive force keeps the particles dispersed. A dispersed suspension may flow well through the deposition nozzle, but it cannot be used as the robocasting ink because it cannot maintain its shape during printing. Thus, the disperse sol must be flocculated to obtain a paste with yield stress and shear thinning character. **Figure 1.2** is an idealized schematic of an ink formulation consisting of spherical particles in an aqueous solution.[14,17] The dispersed particle can be flocculated by pH change and the addition of a binder.

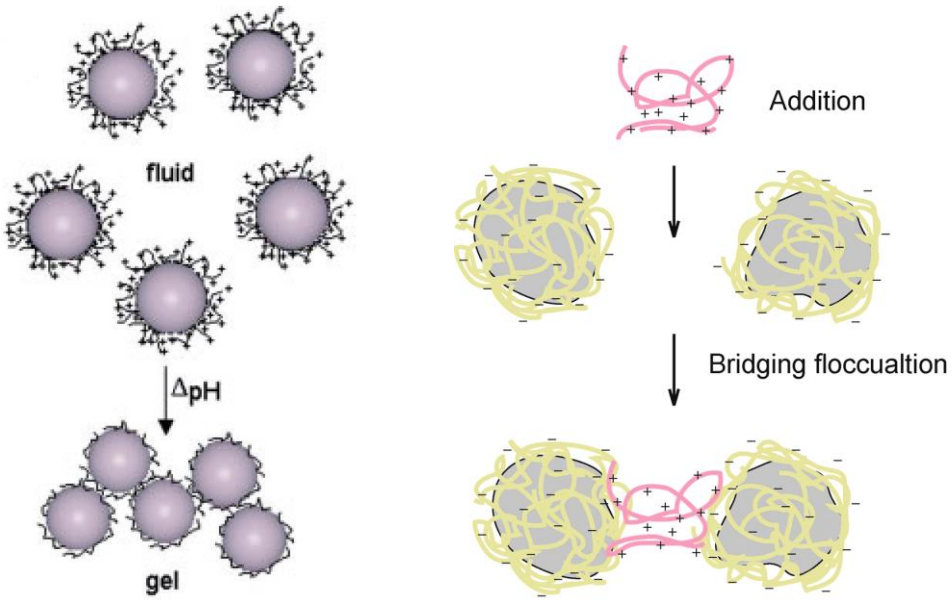

(a) (b)

Figure 1.2 Schematic illustration of the ink formulation concept induced by a) pH change, b) bridging flocculation[14,17]

1.2 Electrochemical Reduction process of Titanium dioxide

1.2.1 Titanium reduction process

Titanium is the ninth most abundant element on the surface of the earth and it is also the fourth most abundant element in metal resources. Titanium is found in nature as titanium dioxide (TiO_2) in three mineral forms as rutile, anatase, and brookite of which rutile is the most common. The rutile crystal structure is tetragonal. Crystallites have acicular to prismatic character. Anatase is also common with tetragonal crystal structure and pyramidal shape. Brookite is an orthorhombic form of TiO_2 and is rare in comparison to rutile and anatase. The density of titanium metal is low at 3.7 g/cm^3. Titanium is

mainly used as an aerospace frame material because it is a light weight and strong. Also among its many uses, titanium metal and alloys of titanium are used in turbine fan blades for aircraft, piping for chemical reactors, and biomedical implants. The oxides of titanium are used as a catalyst for chemical reactions for producing olefin and hydrogen.

Titanium was discovered in the 18th century by Gregor and Klaproth based on the experimental investigation of sample ores.[19] Gregor discovered Ti in ilmenite sand and Klaproth tested rutile. In 1910, Mattew fabricated intermediate pure titanium through the reaction of $TiCl_4$ and Na. In 1925, van Arkel and de Boar made high purity titanium[20] by decomposition of TiI_4 on a high temperature filament. In 1940, Kroll[21] patented a process for production of high purity titanium by the reduction of $TiCl_4$ using magnesium. The Kroll process is the dominant current method to produce high purity titanium used in industry. Although the Kroll process is widely used it suffers from slow reaction kinetics, expensive and complex refining steps, and safety issues.

1.2.2 Commercial Process for Ti Production

The industrial methods of Ti production from TiO_2 ore consists of two steps: 1) Production of $TiCl_4$ and 2) reduction of $TiCl_4$ with Na or Mg. The chlorination[22-24] from rutile is critical to the process in these steps. **Figure 1.3** shows several Ti producing processes in use today.[25] Each process has four stages: raw material, impure intermediates, pure intermediates and product. $TiCl_4$ can be produced by contact with Cl_2 gas with TiO_2 as in the following exothermic equation:[26,27]

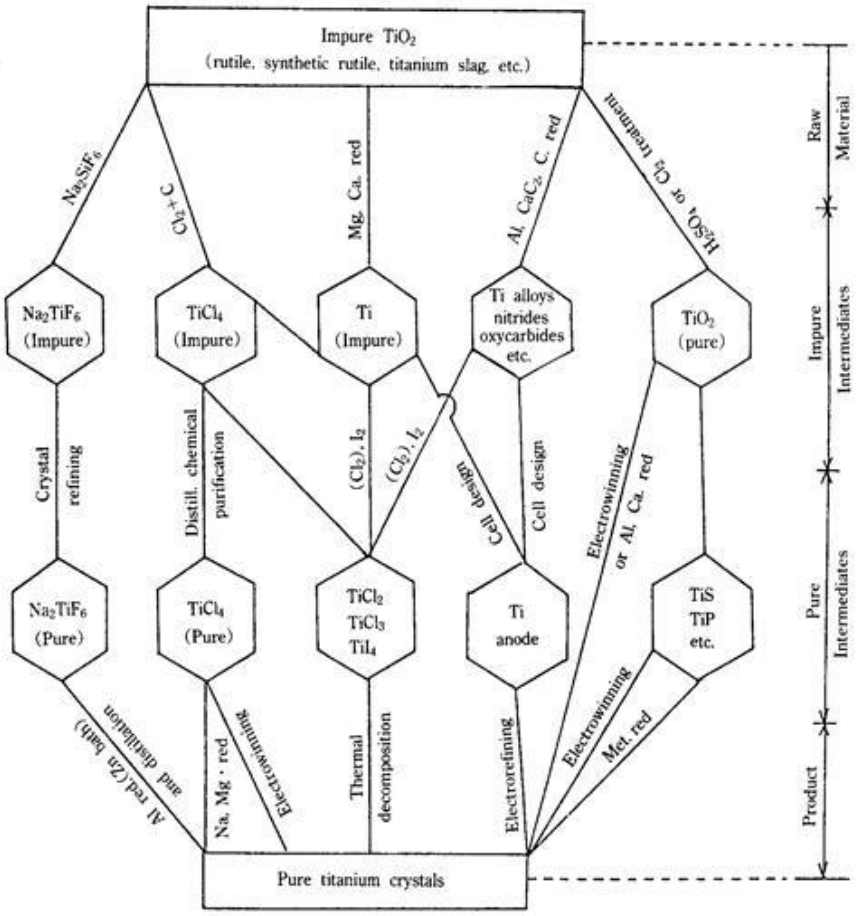

Figure 1.3 Example routes of commercial titanium processing[25]

$$TiO_2 + 2Cl_2 + 2C \rightarrow TiCl_4 + 2CO \qquad \Delta G = \text{-}10.9 \text{ kcal at } 1000°C \qquad (1.2)$$

$$TiO_2 + 2Cl_2 + C \rightarrow TiCl_4 + CO2 \qquad (1.3)$$

The purity of $TiCl_4$ is very important in this process. If impurities such as CaO and MgO exceed 1 %, the chlorination of rutile will not succeed. These produced impurities remain in the liquid phase at high temperature and they obdurate the exit of the produced gas. Also, CaO produces CaO-TiO_2 and it interrupts the chlorination of TiO_2. $TiCl_4$ is a very stable compound, and its decomposition reaction is as follows[26,27]:

$$TiCl_4 \rightarrow Ti + 2Cl_2 \qquad \Delta G = +175{,}600 - 29.11T \text{ kcal} \qquad (1.4)$$

The decomposition reaction can be successful only at extremely high temperatures and is impractical for commercial purposes. There are three common reduction methods employed: reduction using Mg, Na and electro winning. The reduction process using Mg was suggested by Kroll (4) and its reaction mechanism is as follows[26,27]:

$$TiCl_4(gas) + 2Mg(liq) \rightarrow Ti(Solid) + 2MgCl_2(liq)$$
$$\Delta G = -762 kcal/mol \text{ at } 900^{o}C \qquad (1.5)$$

The reduction process using Na is suggested by Hunter. [28,29] This reaction is very similar to the Kroll process except that the reaction mechanism consists of two steps. This reaction is carried out at 900℃ and it has -270 kcal/mol enthalpy. Gibbs free energy of this reaction is -143 kcal/mol.

$$TiCl_4(gas) + Na(liq) \rightarrow TiCl_2(solid) + 2NaCl(liq) \quad (1.6)$$

$$TiCl_2(solid) + 2Na(liq) \rightarrow Ti(solid) + 2NaCl(liq) \quad (1.7)$$

overall reaction

$$TiCl_4(gas) + 4\,Na\,(liq) \rightarrow Ti(solid) + 4NaCl(liq) \quad (1.8)$$

Electrorowinning was first introduced for titanium production in 1954 by Rand, M.j et al.,[30] Leone O. Q et al.,[31] suggested an electrowinning process which used LiCl and KCl electrolyte. The electrolyte mixture is melted at high temperature and it is used as an electrolyte with $TiCl_4$ added. The major reaction mechanism is as follows[31] :

Anode

$$2Cl^-(\ell) \rightarrow Cl_2(g) + 2\,e^- \quad (1.9)$$

Cathode with feeding $TiCl_4(g)$

$$Ti^{+4} + 2e^- \rightarrow Ti^{+2} \quad (1.10)$$

Cathode with exiting Ti

$$Ti^{+2} + 2e^- \rightarrow Ti \quad (1.11)$$

In 1971, Hashimoto et al.,[32-34] studied electrowining of pure titanium using titanium oxide and other mixed oxide such as TiO_2, $FeTiO_3$, $CaTiO_3$ and $MgTiO_3$ within molten salts such as CaF_2, MgF_2, BaF_2, and NaF. In 1987, Cinattaet al.,[35] made a new electrowining process.

1.2.3 Direct Electrochemical Reduction of Titanium Dioxide in Molten Calcium Chloride

In 2000, Fray et al.,[36,37] patented a process called the FFC process. It is an electrochemical reduction process using TiO_2 in molten calcium chloride ($CaCl_2$). The TiO_x remains in the solid state throughout the process such that the final Ti product has the same shape as the starting ceramic pellet. In developing the FFC process, two different configurations of the reduction systems were tried. One system had TiO_2 pellets placed into a graphite crucible with molten $CaCl_2$. A graphite rod was used as the anode and the graphite crucible was used as the cathode. The second system used kanthal wire as the cathode and the TiO_2 pellets were fixed on the wire. A graphite rod was used as the anode. In both configurations, molten $CaCl_2$ was used as an electrolyte. A potential of supplied voltage was 2.8~3.2 V to the electrolytic cell. The reaction was carried out at 700 to 900 ℃ for 1 to 340 hours. After the reaction, analysis using scanning electron microscopy (SEM) and energy dispersive X-ray spectroscopy (EDS) confirmed that TiO_2 was changed to pure Ti.

Fray et al.,[38] also identified the kinetic pathway in the electrochemical reduction of TiO_2 in molten calcium chloride. He used three different stages to determine the kinetic pathway. In the first stage 2.5 V was applied to the reduction system and maintained for 8 hours. In the second stage, 2.7 V was applied to the system and maintained for 24 hours. In the final stage, 2.9 V was applied and maintained until reduction was completed. The reduction process is carried at 900 ℃ for 120 hours. Samples were collected at each stage

and those samples were washed into 1N HCl solution to remove all impurities on the surface of the pellets.

Figure 1.5 shows the current change by experimental reduction time that Fray et al., used to find the reduction mechanism of TiO_2 in FFC method.[38] It was analyzed with SEM and X-ray Diffraction (XRD). Finally, he determined the kinetic pathway in the electrochemical reduction of titanium dioxide in calcium chloride electrolyte. After the analysis, Fray et al., suggested three reaction steps for the TiO_2 dioxidation. In the first stage, the electrochemical reduction of TiO_2 at cathode is suggested as follows[38] :

$$5TiO_2 + Ca^{2+} + 2e^- = Ti_4O_7 + CaTiO_3 \qquad E^0 \approx +1807\,mV \quad (1.12)$$

$$4Ti_4O_7 + Ca^{2+} + 2e^- = 5Ti_3O_5 + CaTiO_3 \qquad E^0 = +1678\,mV \quad (1.13)$$

$$3Ti_3O_5 + Ca^{2+} + 2e^- = 4Ti_2O_3 + CaTiO_3 \qquad E^0 = +1575\,mV \quad (1.14)$$

$$2Ti_2O_3 + Ca^{2+} + 2e^- = 3TiO + CaTiO_3 \qquad E^0 = +1200\,mV \quad (1.15)$$

TiO_2 molecules react with Ca^{2+} ion and produce titanium suboxide (Ti_xO_y) and calcium titanate ($CaTiO_3$). This reaction is continued until TiO_2 converts to oxide (TiO) and calcium titanate ($CaTiO_3$). The accurate value of the cell potential energy for this reaction is given in the equation. However, the cell potential energy for the equation (1.12) is an approximate value because Ti_4O_7 and $CaTiO_3$ are produced through several steps and various Magnoli phase compositions [40] involved in this reaction from TiO_2 to Ti_4O_7.

The second stage of this electrochemical reduction process was also suggested by Fray et al.[38] After the 32 hours reaction the sample was analyzed by SEM and XRD. The amount of TiO and $CaTiO_3$ molecules were dramatically decreased and $CaTi_2O_4$ molecules newly appeared and dominated the surface of sample. Frey et al., suggested two possible reaction pathways in this stage. [38]

$$CaTiO_3 + TiO = CaTi_2O_4 \qquad (1.16)$$

$$2CaTiO_3 + 2e^- = CaTi_2O_4 + Ca^{2+} + 2O^{2-} \qquad E^0 > -146\,mV \qquad (1.17)$$

The first reaction (equation (1.16)) is the redox reaction between TiO and $CaTiO_3$ because it takes place chemically without changing the oxidation state of the titanium and the current is not considered in the reaction. The second equation (equation (1.17)) is the oxygen removal reaction on the cathode. The first reaction is the most dominant reaction in this stage and the second reaction is not spontaneous because the cell potential value is negative, despite the fact, it is cathode reaction.

The third stage of the electrochemical reduction is the decomposition of $CaTiO_4$ on the cathode. TiO is produced and Ca^{2+} and O^{2-} are also released in this stage.

$$CaTi_2O_4 + 2e^- = TiO + Ca^{2+} + 2O^{2-} \qquad E^0 < +417\,mV \qquad (1.18)$$

The removal of the oxygen ion from TiO is expected in the cathode reaction. The generated oxygen ions are transferred to the anode side and react with carbon or carbon oxide.

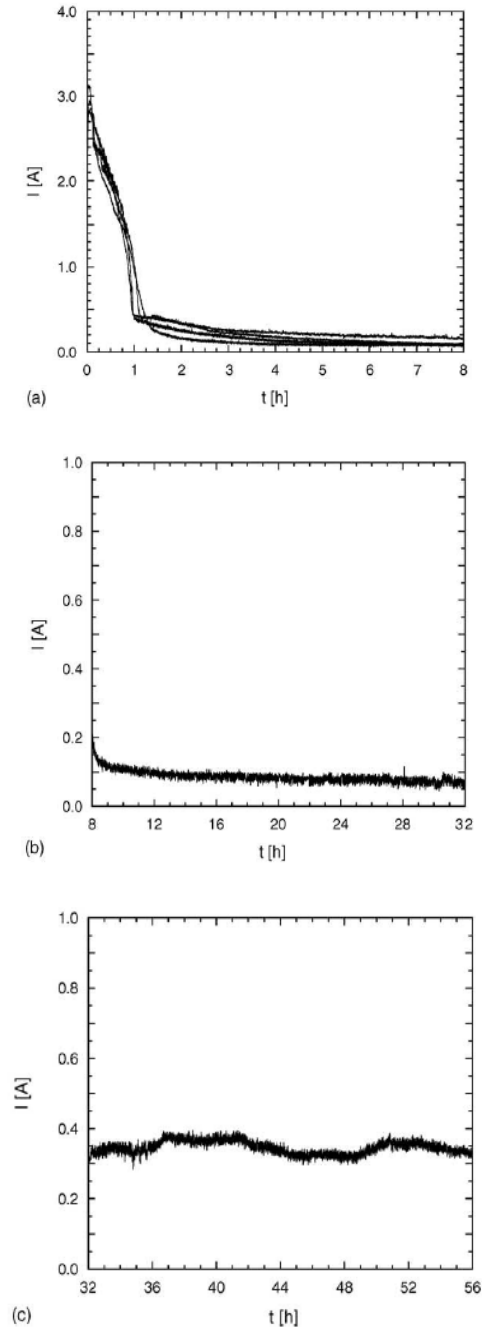

Figure 1.4 Current vs. time curves of electrochemical reduction experiments. Electrolyte: calcium chloride; cathode: titanium dioxide pellets (mass 8 g); anode: graphite (geometric surface area 12 cm2); anode-to-cathode distance: 4 cm; temperature: 900 ˚C; atmosphere: dried argon. (a) Four nominally identical experiments performed at a voltage of 2.5V; (b) continuation of one of the experiments at a voltage of 2.7 V; (c) continuation of the same experiment at a voltage of 2.9 V. [38]

$$TiO + 2(1-\delta)e^- = Ti[O]_\delta + (1-\delta)O^{2-} \qquad E^0 \approx +117\,mV \qquad (1.19)$$

The intermediate products from this FFC method are reported by K. T. Jacob and Sapna Gupta.[39] **Table 1.1** and **Figure 1.5** show the identified intermediate product of the phase diagram in Ca-T-O system at 1200 ^oC. In the research, they changed the molar ratio of Ti, TiO_2, Ti_2O_3 and Ca. Although the reaction condition was the same, the product was different by the added molar ratio. The high molar ratio of Ti and Ti_2O_3 mixture (over 40%) produce Ti(α) and Ti(β). However lower Ti ratios were not produced Ti metals.

The reactions on the anode side are also suggested. Chlorine gas, oxygen, carbon monoxide and carbon dioxide are produced in the anode side and it is shown in the following equations [38]:

$$Cl_2 + 2e^- = 2Cl^- \qquad E^0 = +3214mV \qquad (1.20)$$

$$\frac{1}{2}O + 2e^- = O^{2-} \qquad E^0 = +2407mV \qquad (1.21)$$

$$CO + 2e^- = C + O^{2-} \qquad E^0 = +1291mV \qquad (1.22)$$

$$\frac{1}{2}CO_2 + 2e^- = \frac{1}{2}C + O^{2-} \qquad E^0 = +1381mV \qquad (1.23)$$

As shown in the reduction equations, the reduction carbon monoxide and carbon dioxide have lower cell potential. When these reactions occur in the oxidation direction, the generation of CO and CO_2 are preferred at lower magnitude cell voltages. However, if the cell potential is made sufficiently low, the generation of Cl_2 gas can occur. It generate

Table 1.1 Starting materials, average composition of the sample and phase identified after equilibration in the system Ca–Ti–O at1200 K.[39]

Sample number	Starting materials	Average composition of samples			Phases identified	Techniques used
		X_{Ca}	X_{Ti}	X_O		
1	$Ca + Ti_2O_3$	0·50	0·20	0·30	$Ca + Ti(\beta) + CaO$	XRD, SEM, EDS
2	Ca + TiO	0·40	0·30	0·30	$Ca + Ti(\beta) + CaO$	XRD, SEM, EDS
3	$Ca + Ti + Ti_2O_3$	0·30	0·40	0·30	$Ti(\beta) + CaO$	XRD
4	$Ca + Ti + Ti_2O_3$	0·28	0·42	0·30	$Ti(\beta) + CaO$	XRD
5	$Ca + Ti + Ti_2O_3$	0·20	0·50	0·30	$Ti(\beta) + Ti(\alpha) + CaO$	XRD, SEM, EDS
6	$Ca + Ti + Ti_2O_3$	0·20	0·40	0·40	$Ti(\alpha) + CaO$	XRD
7	$Ca + Ti + Ti_2O_3$	0·16	0·40	0·44	$Ti(\alpha) + TiO + CaO$	XRD, SEM, EDS
8	$CaO + Ti + TiO_2$	0·30	0·20	0·50	TiO + CaO	XRD, SEM, EDS
9	$CaO + Ti + Ti_2O_3$	0·30	0·20	0·50	TiO + CaO	XRD, SEM, EDS
10	$CaO + Ti + TiO_2$	0·20	0·27	0·53	$TiO + CaO + CaTi_2O_4$	XRD, SEM, EDS
11	$CaO + TiO_2$	0·35	0·10	0·55	$CaO + Ca_3Ti_2O_7$	XRD
12	$CaO + Ti + TiO_2$	0·29	0·16	0·55	$CaO + Ca_3Ti_2O_7 + CaTi_2O_4$	XRD, SEM, EDS
13	$CaO + Ti + TiO_2$	0·25	0·20	0·55	$CaO + CaTi_2O_4$	XRD
14	$CaO + Ti + TiO_2$	0·10	0·35	0·55	$CaTi_2O_4 + TiO$	XRD, SEM, EDS
15	$CaO + Ti + TiO_2$	0·13	0·30	0·57	$CaTi_2O_4 + TiO_{1+x}$	XRD, SEM, EDS
16	$CaO + Ti + TiO_2$	0·10	0·33	0·57	$CaTi_2O_4 + TiO_{1+x} + CaTiO_3$	XRD, SEM, EDS
17	$CaO + Ti + TiO_2$	0·21	0·21	0·58	$Ca_3Ti_2O_7 + Ca_4Ti_3O_{10} + CaTi_2O_4$	XRD, SEM, EDS
18	$CaO + Ti + TiO_2$	0·21	0·20	0·59	$Ca_4Ti_3O_{10} + CaTiO_3 + CaTi_2O_4$	XRD, SEM, EDS
19	$CaO + Ti + TiO_2$	0·10	0·30	0·60	$CaTiO_3 + Ti_2O_3$	XRD, SEM, EDS
20	$CaO + Ti + TiO_2$	0·10	0·29	0·61	$CaTiO_3 + Ti_2O_3 + Ti_3O_5$	XRD, SEM, EDS
21	$CaO + TiO_2$	0·125	0·25	0·625	$CaTiO_3 + TiO_2$	XRD
22	$TiO_2 + Ca_4Ti_3O_{10}$	0·125	0·25	0·625	$CaTiO_3 + TiO_2$	XRD

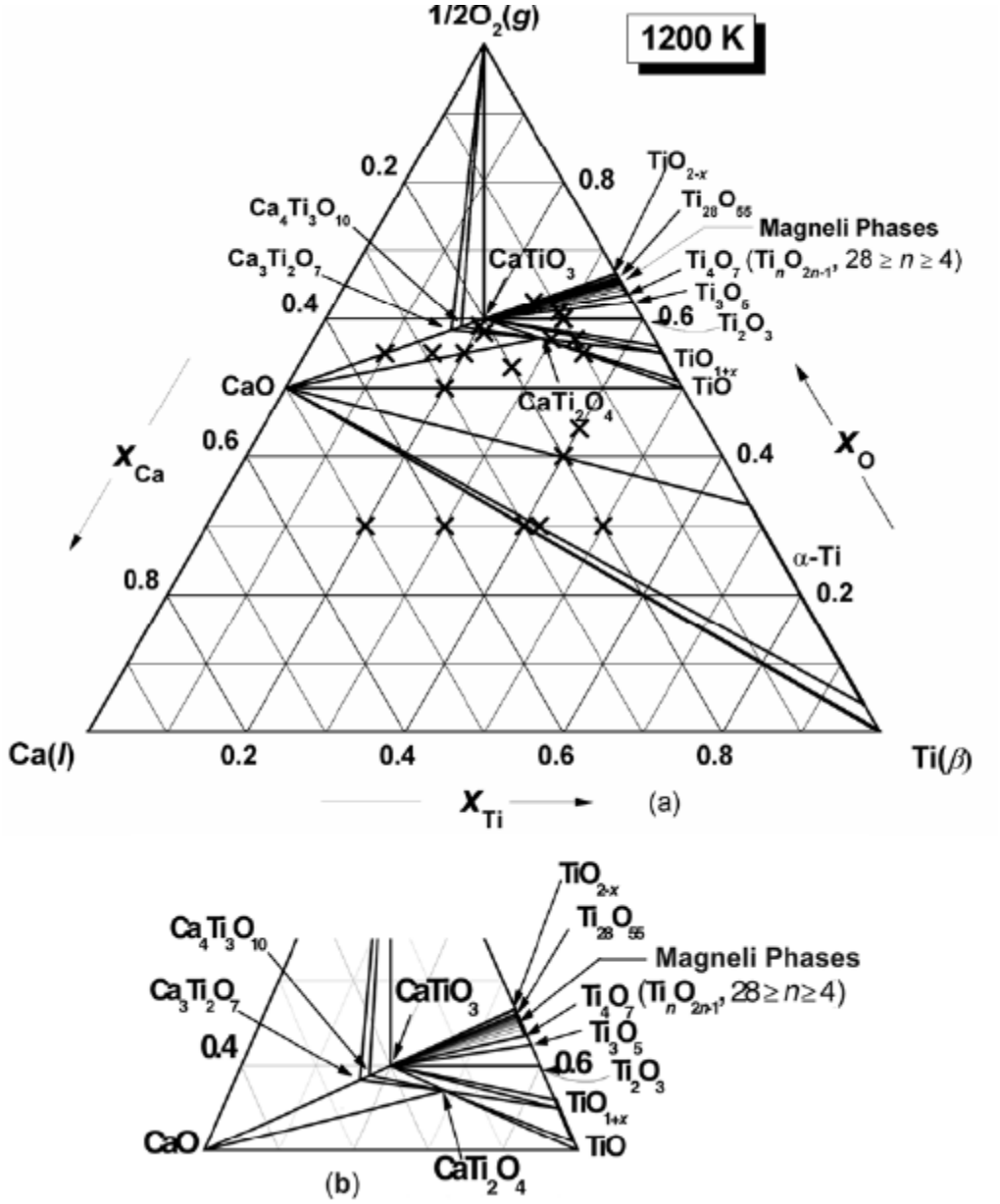

Figure 1.5 (a) An isothermal section of the phase diagram for the system Ca–Ti–O at 1200 K composed from the results of this study and (b) an expanded view of the diagram between XO = 0·5 and XO = 0·73[39].

about 3.2 volts, thus if the system controlled over the volts, the consumption of molten $CaCl_2$ will occur during the reduction process. Addition, the generated Cl_2 gas can react with other materials such as metal wire and quartz housing, critically damaging the system.

1.2.4. Determining Cell Potentials

The zero current cell voltage can be calculated for the electrochemical reduction process and reactions on anode and cathode can be predicted by this step. The method to calculate cell potential is similar to that using the Gibbs free energy. If the designed reaction mechanism is unfavorable in thermodynamics, the cell potential is also unfavorable. Thus, we can predict reaction mechanism in anode and cathode sides.

The cell potential energy equation has same formula with gibbs free energy equation. The standard state (1molar concentration of ions in solution, 1 atm of pressure, and T=25 $^{\circ}$C) cell potential is:

$$E^{O}_{cell} = E^{O}_{reduction} + E^{O}_{oxidation} \tag{1.24}$$

The non-standard state potential can be calculated with the Nernst equation:

$$E_{cell} = E^{O}_{cell} - (\frac{RT}{nF}) \ln Q \tag{1.25}$$

Where;

E_{cell} = cell potential at non standard state conditions

E^{O}_{cell} = cell potential at standard state conditions

R = Gas constant (J/mole K)

T = temperature (K)

F = Faraday's constant (C/mole e^-)

n = number of electron moles that transferred in the designed reaction mechanism

Q = reaction quotient

In this research, 3-D lattice structures are used for the electrochemical reduction process (FFC method). A TiO_2 paste is produced and characterized by rheologic measurements and is used in the robocasting method to fabricate the 3-D lattice structure. The electrochemical reduction process was carried out using two different conditions. In the first method (control), the normal FFC condition of constant voltage and variable current verified the expected reaction pathway as previously reported. The second condition (test) uses a constant current and variable voltage. Under the test condition, TiO fibers are produced as an intermediate product. Fibers of metal oxides have been of increasing interest due to large surface area to volume ratio for catalysis and for improved mechanical properties. For Ti-based oxides (typically TiO_2), nanofibers are produced by electrospinning[41,42] and the sol-gel method. [43] However, we find no reference to fabrication of TiO fibers despite some potentially interesting properties. TiO has a wide homogeneity range from $TiO_{0.75}$ to $TiO_{1.3}$ in composition. [44] TiO can accommodate a large number of O^{2+} vacancies and Ti can have 4+ and 3+ oxidation states. TiO is

electronic conductor with a resistivity of about 3 x 10^{-3} Ωcm. The properties of TiO fiber are still unknown, thus the study to find the properties must be carried out to widen its application. Furthermore the fabrication mechanism for the TiO fiber should be carried out as well in order to control its size and length.

CHAPTER 2 EXPERIMENTAL METHOD

2.1 Three Dimensional Printing

TiO_2 powder (rutile, sigma-aldrich 14021) is printed into a three-dimensional lattice structure using a solid freeform fabrication technique called Robocasting. For brevity, the printed and lightly sintered structure will be referred to as a "pellet". For printing, the TiO_2 powder is mixed into an aqueous solution of polyethylenimine (PEI, Aldrich, Mn=1200). The TiO_2 content of the mixture is 37% by volume. The PEI content in the suspension is based on TiO_2 weight at a ratio of 26 mg PEI per gram of TiO_2. This suspension has low viscosity indicating a well-dispersed ceramic slurry. Next, hydroxypropyl methylcellulose (Methocel F4M, Dow Chemical), from a 5% aqueous stock solution is added to achieve a final concentration of 0.5% in the liquid phase. Finally, ammonium poly acrylate (Darvan 821A, R.T Vanderbilt Co. Inc) is added drop-wise to the suspension to gel the PEI coated TiO_2 colloids and to create a paste that can be extruded.

The paste is then loaded into a 3mL syringe on the Robocasting machine (custom x,y,z gantry robot) and extruded as a 0.2mm diameter filament while the machine traces a pre-defined pattern in the x-y plane to create a parallel line pattern with the extrudate. Multiple layers are printed, on top of each other, to create a three-dimensional lattice. After printing, the structure is dried in ambient air and then sintered at 1100 $^{\circ}$C for 7 hours in a furnace, followed by cooling to room temperature. The process flow diagram for TiO_2 3-D printing is shown in **Figure 2.1**.

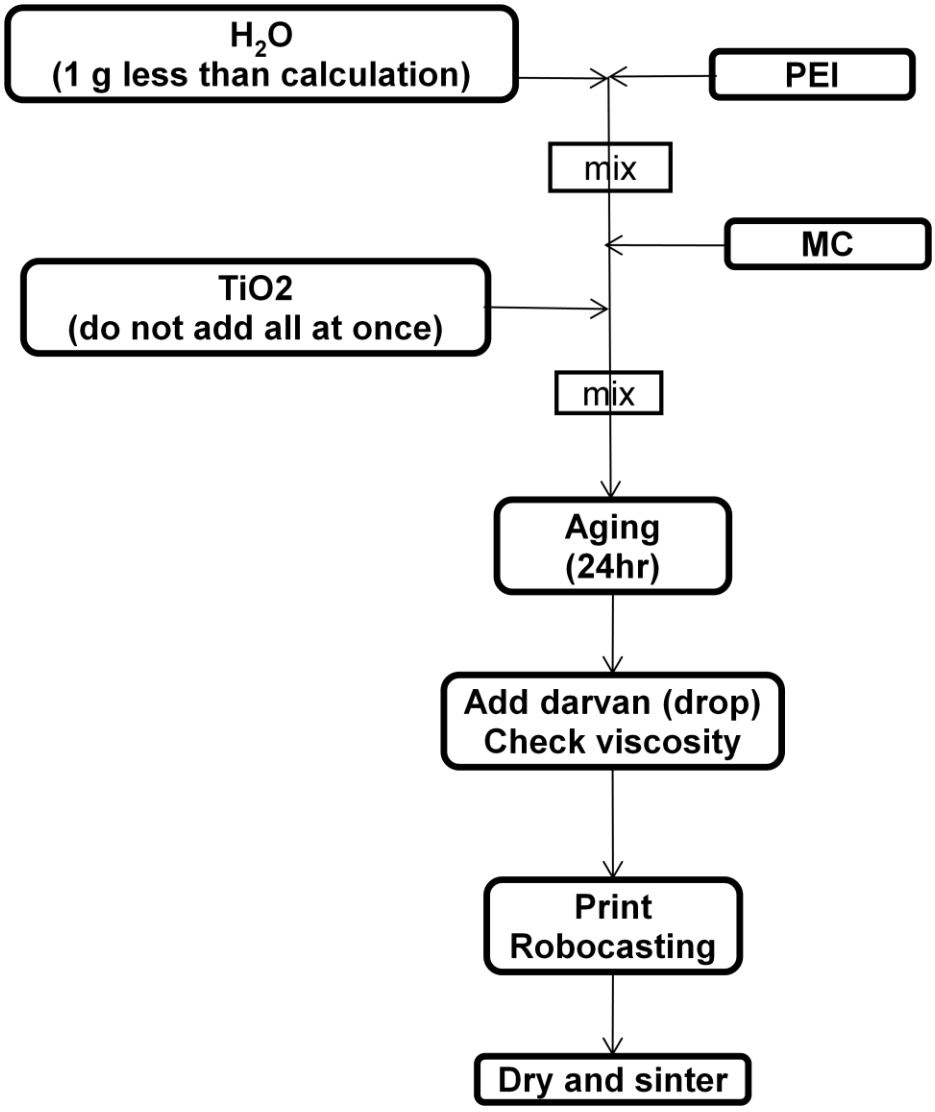

Figure 2.1 The schematic diagram of robocasting for 3-D printing

2.2 Electrochemical Reduction (FFC process)

The lightly sintered TiO_2 pellet is placed in the bottom of a graphite crucible and covered with $CaCl_2$ salt granules. The crucible is placed inside a quartz housing with a lid. The quartz housing is placed inside a box furnace (Lindberg/BlueM : BF51866A-1) and an opening in the lid is piped to a hole in the top of the furnace for connection of argon gas and electrodes. One of the electrodes is a graphite rod connected to a chromolly wire. The other electrode is a chromolly wire connected to the graphite crucible. The graphite rod (anode) and crucible (cathode) are connected to a power supply (HP, 6214A). Argon gas is also connected to the inner quarts tube and flows to the crucible. The voltage is controlled by the power supply and the current is determined by the overall reaction rate in the electrolytic cell and resistance of the experimental setup and it is measured by an ammeter (Omega HM331 Multimeter, Omega Instruments). A schematic diagram of the electrochemical reduction system is shown in figure 2.2.

The temperature is increased upto 950 ℃ in several steps (140 ℃ 1 hr, 450 ℃ 1hr). When the temperature reaches 950 ℃, the electrical circuit is connected between the anode and cathode. Two experimental conditions are tested with separate pellets. In the first, the electrical potential is fixed at 3.2 V and the current is allowed to vary (monotonic decrease) through the first 18 to 24 hours of reaction. In the second case, the voltage is increased from 2.5 to 4.2 V during the first 24 hours while holding current. After the 24 hours of reaction in the second case, the current did not decrease and the voltage was kept at 4.2 V until the reaction was stopped. The voltage and current control is shown in **Figure 2.3**.

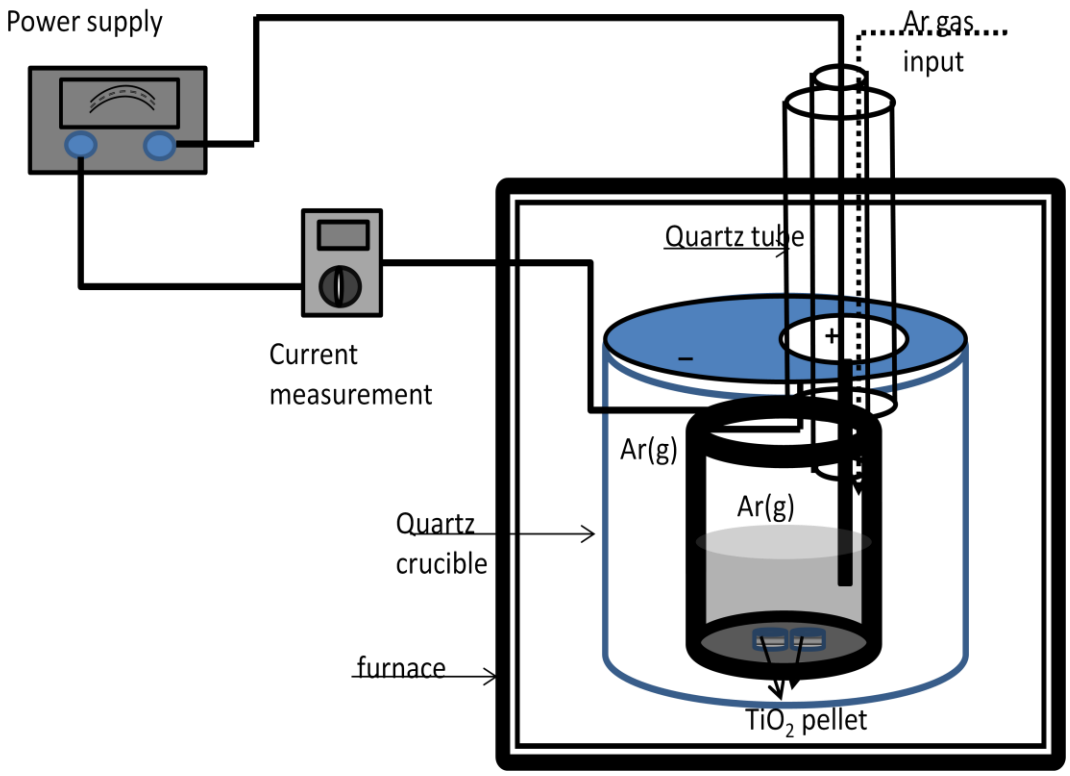

Figure 2.2 schematic diagram of the electrochemical reduction of the TiO_2 pellet; the graphite crucible is connected to the cathode and the graphite rod is connected to the anode. Argon gas was continuously purged.

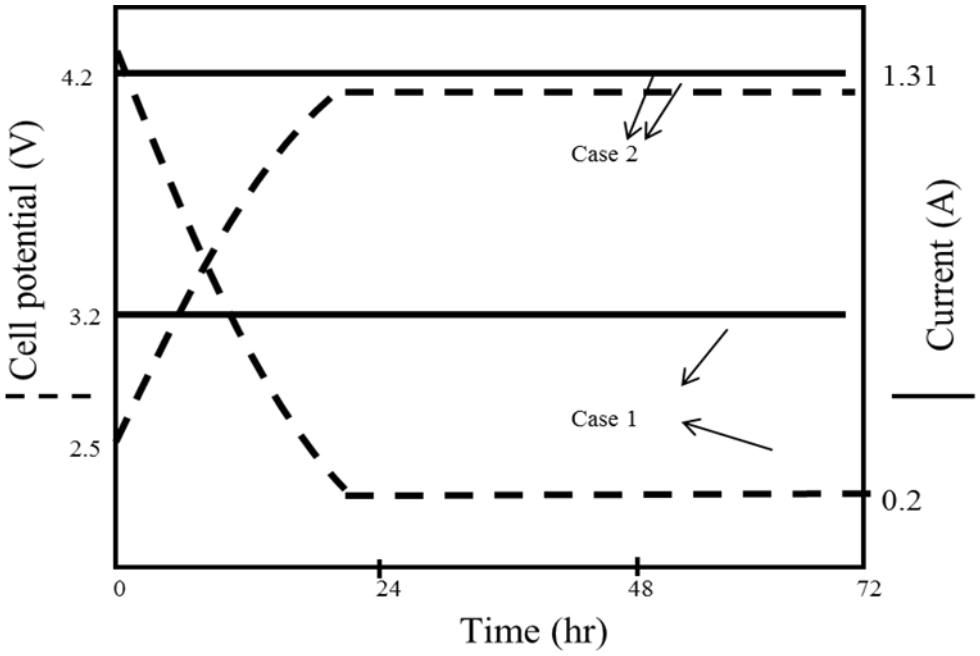

Figure 2.3 Voltage and current control for the electrochemical reduction process.

2.3 Characterization

At various stages of preparation (as-sintered, short reaction time, long reaction time, etc.) representative pellets are prepared for scanning electron microscopy by gold sputtering and placed in the SEM (JEOL 6360) for general observation of morphology of particles in the lattice rods. A similar pellet is carbon coated for energy dispersive X-ray spectroscopy (EDS, FEI Quanta 600) analysis. In EDS characterization, Ti and Ca element mapping are used to discern the distribution of these elements in the observed structure. At select points in the structure, quantitative chemical analysis by EDS is performed. The bulk phase composition of the pellet is measured by X-ray diffraction (XRD, Bruker D8 Discover) using Cu kα radiation and a two-theta range from 3^{o} to 95^{o}.

CHAPTER 3 EXPERIMENTAL RESULTS

3.1 Optimization of Titanium Dioxide Ink for Robocasting

The dispersion of TiO_2 powder in water is one of the most critical steps in production of ink for robocasting. A properly dispersed suspension of TiO_2 should have low viscosity and some shear thinning character. This rheology is best measured using a Couette cell on a controlled stress rheometer. Figure 3.1 shows the measurement of the shear rate ($\dot{\gamma}$) and apparent viscosity ($\eta_{app} = \tau/\dot{\gamma}$) as a function of increasing shear stress (τ) and dispersant concentration using a 14 mm diameter bob in a 14.25 mm diameter cup Couette cell. The poly(ethylenimine) was changed from 2.1 % to 2.8 % based on TiO_2 powder weight while the volume fraction of TiO_2 was held constant at a value of ϕ=0.35.

At low PEI content (i.e., less than 2.4%) the suspension displayed properties of a gel with a finite yield stress and little flow before that magnitude of stress is achieved. Above this concentration, the TiO_2 suspension showed a low-shear Newtonian plateau followed by a shear thinning region and a high shear Newtonian plateau. The two Newtonian plateaus with an intermediate shear thinning region is characteristic of a well-dispersed colloidal system at high volume fraction solids. It was determined that a PEI content of around 2.5% to 2.6% was sufficient to disperse the TiO_2 particles and that an excess of PEI simply remained in the solution and did not contribute to further dispersion.

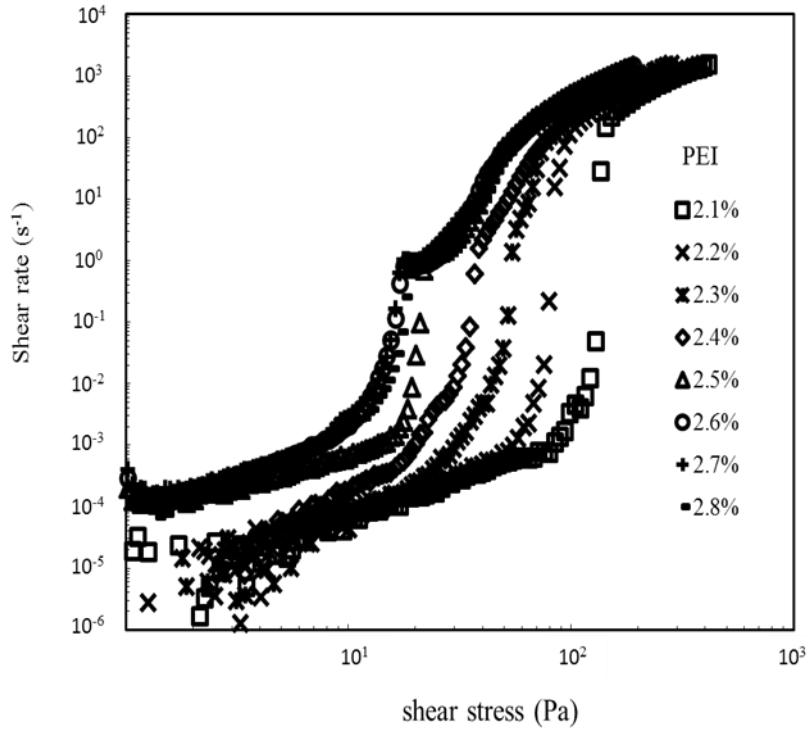
Shear rate (s-1)
shear stress (Pa)
PEI
2.1%
2.2%
2.3%
2.4%
2.5%
2.6%
2.7%
2.8%

(a)

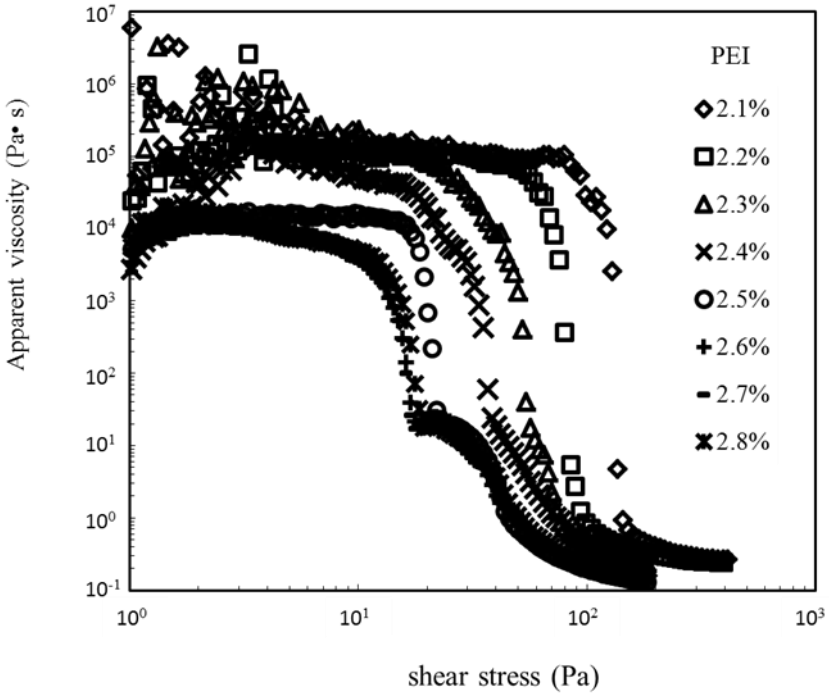
Apparent viscosity (Pa• s)
shear stress (Pa)
PEI
2.1%
2.2%
2.3%
2.4%
2.5%
2.6%
2.7%
2.8%

(b)

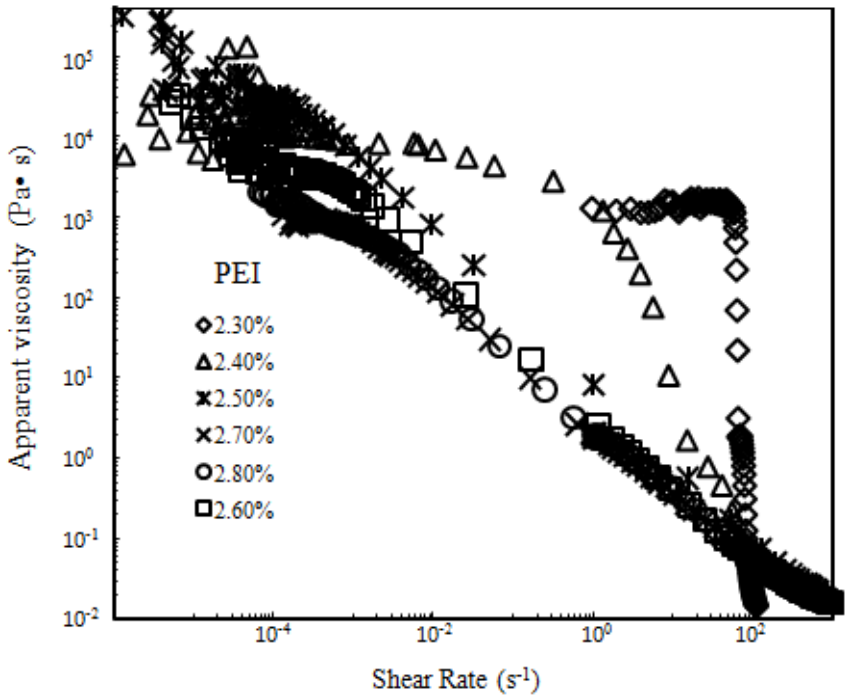

(c)

Figure 3.1 The (a) shear rate and (b) apparent viscosity as a function of shear stress PEI (wt% per wt TiO_2) rate change (c) apparent viscosity as a function of shear rate PEI rate change; TiO2 powder was fixed TiO_2 powder volume at 35 % in total volume.

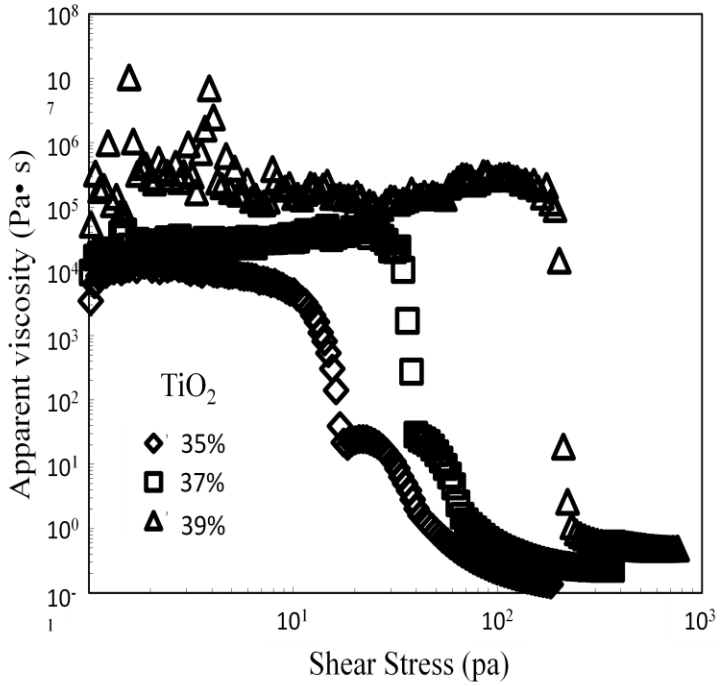

(a)

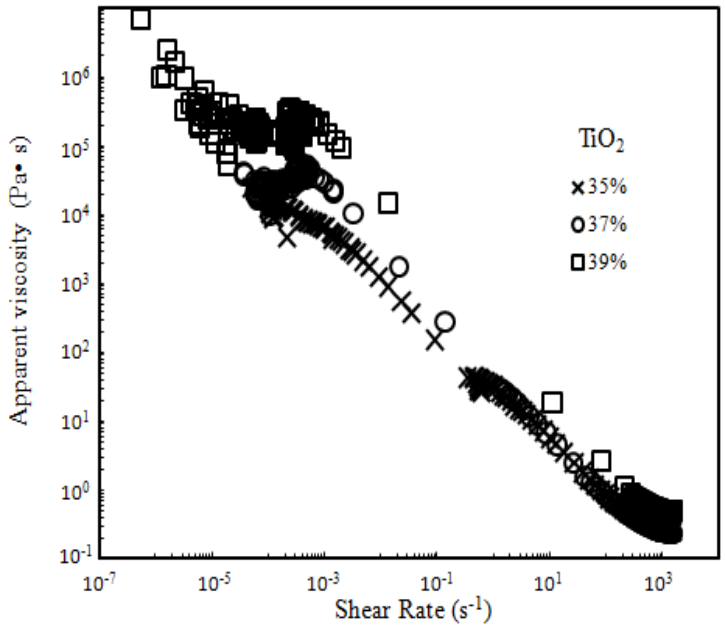

(b)

Figure 3.2 Instantaneous viscosity as a function of shear stress(a) and shear rate (b) for various TiO_2 volume fraction suspension having fixed PEI content of 2.6 % based on TiO_2 weight.

In **Figure 3.2**, the effect of increasing solids volume fraction on the viscosity of TiO_2 suspensions is shown. As expected, an increase in solids volume fraction increases the viscosity of the suspension at all shear rates. For the purpose of this study, a volume fraction of 0.37 was chosen as a comfortable ink formulation with satisfactory flow properties (i.e., well-dispersed, low-viscosity suspension) to serve as a starting point for the colloidal gel.

3.2 Sintering of 3-D Structure Titanium Dioxide

The process of robocasting has been well-described in the previous literature and was simply used in this work to produce 3-D lattice structure. The printing sequence is illustrated in **Figure 3.3** where the lattice is a repeat of two orthogonally oriented sets of lines confined within a circular region. The layers are repeated to build up the three dimensional lattice. Several lattices were printed, dried and sintered in preparation for the electrochemical reduction process.

Figure 3.4 shows scanning electron microscopy (SEM) images of representative portions of as-sintered TiO_2 lattices after seven hours of sintering. The image is a close view of the surface of one of the lattice rods. As the temperature was increased, the particle size increases, and the porosity decreased. Ceramic sintering is a process that depends greatly on time and temperature. A sintering temperature of 1100 ˚C for seven hours was determined to provide sufficient strength and porosity for the subsequent electrochemical reaction. The electrochemical reduction process causes particle

Figure 3.3 The schematic illustration of printing sequence for robocasting

Morphology changes and can leave the filaments of the lattice structure weakened and fragile. However, if the porosity is insufficient in the initial pellet, the electrolyte cannot penetrate the filament and the active electrode area is small. Hence, a compromise was reached between fully dense and strong versus very porous and weak. **Figure 4(a)** shows an insufficiently sintered microstructure that is too weak for further processing while **Figure 4(c)** shows a lattice with insufficient porosity in the lattice filaments. Figure 4b is the case of sintering for seven hours at 1100 ^{o}C and this structure showed good strength and sufficient interconnected porosity.

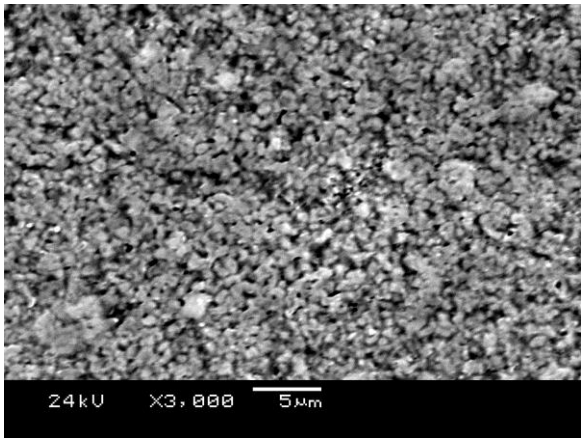

(a)

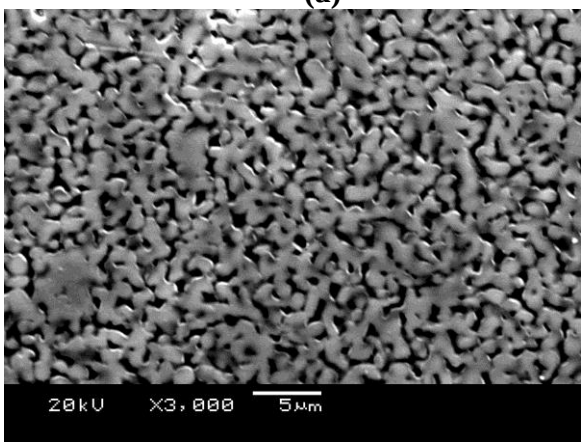

(b)

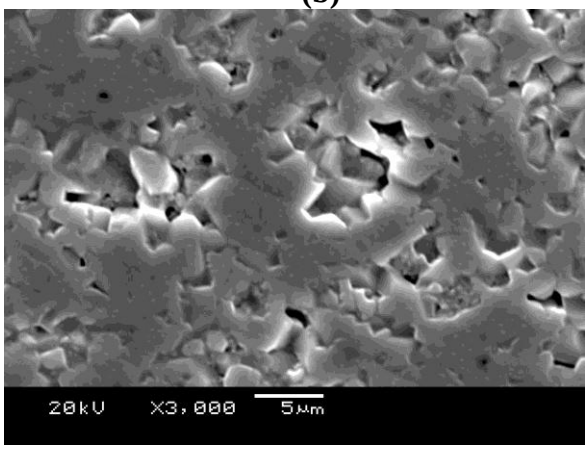

(c)

Figure 3.4 SEM image of TiO_2 lattice surfaces after 7 hr sintering ; (a) 1000 ˚C, (b) 1100 ˚C, (c) 1200 ˚C

3.3 Electrochemical Reduction of Titanium Dioxide

The TiO_2 reduction process involves several reaction steps and produces many intermediate products such as titanium sub-oxide and calcium titanate. [16,17] **Figure 5** shows these TiOx and $CaTiO_3$. **Figure 5(a)** is an observation after 24 hours of reduction and **Figure 5(b)** after 72 hours of reduction. 3.2 voltage power supplied both system at 950 ˚C. In **Figure 5(b),** the large polyhedron particle is calcium titanate and the small cubic particle is TiO. This intermediate product is produced by the reaction between TiO_2, Ca^{2+} and the electron on the cathode side.

There are some differences reaction process between the bottom and top of the pellet as shown in **Figure 3.6**. TiO_2, faced on the graphite crucible, shows a faster reaction process than the upper layer of lattice. Because of this process difference, large $CaTiO_3$ particles are mostly found in the lower layer and TiOx and small $CaTiO_3$ particles are found in the upper layer. Usually the TiO_2 electrochemical reduction process uses densely packed pellets and may help the electron supply of the next TiO_2 particle. As shown in **Figure 3.4**, the particle has lots of pores thus it helps to have wide contact with molten $CaCl_2$. We expected that the wide contact area would make faster TiO_2 reduction. However, most of the processed TiO_2 reduction was found on the bottom of the pellet which was near the graphite crucible. This means that the ion supply next to the pellet is more important than Ca^{2+} contact to pellet in the reduction process. The reaction stopped after 24 hours at 950 ˚C and 3.2 volts was supplied to the system.

TiO_2 reacts with Ca^{2+} and electron and makes TiOx and $CaTiO_3$. The TiOx which composed from the previous reaction, reacts with Ca^{2+} and electron. This reaction is

processed step by step until titanium sub-oxide becomes TiO [38]. Fray et al., [38] reported the intermediate steps. The report says that five mole TiO_2 reacted with one mole Ca^{2+} and two mole electrons and makes Ti_4O_7, TiO and $CaTiO_3$ in the initial step. However, we detected the XRD pattern after 24 hours reduction and it is shown in **Figure 3.6**. Many particles have a higher number of Ti molecules are found. Ti_9O_{17} has the most high mole number of Ti in the XRD titanium sub-oxide patterns. This differs from Fray et al., study. If we analyze the pellet samples with a shorter reduction of 24 hours, higher titanium and oxygen molecule composites would be found.

The reaction path way on the cathode between TiO_2, Ca^{2+} and electron is shown in the equation (3.1). This reaction is continued until the titanium sub-oxide becomes titanium oxide.

$$nTiO_2 + Ca^{2+} + 2e^- = Ti_{(n-1)}O_{2n-3} + CaTiO_3 \qquad (3.1)$$

$$(n-1)Ti_{n-1}O_{2n-3} + Ca^{2+} + 2e^- = Ti_{n-2}O_{2(n-1)-3} + CaTiO_3 \qquad (3.2)$$

Figure 3.7 shows the pellet surface after 72 hours at 950 ^oC electrochemical reduction. 3.2 volts were supplied to the system (case 1). The TiO and $CaTiO_3$ from the first reaction step react together to $CaTi_2O_4$ (redox reaction). The reaction mechanism for this step is already reported and discussed in the introduction section. The square and hexagonal column shape $CaTi_2O_4$ domanates the surface of the pellet. Some of TiO and $CaTiO_3$ which is not reacted with yet are also found in the figure. If the reaction is continued longer, the TiO and $CaTiO_3$ will convert to the $CaTi_2O_4$ and $CaTi_2O_4$ is expected to be converted to Ti metal. The third reaction step is already reported by Fray group.[38]

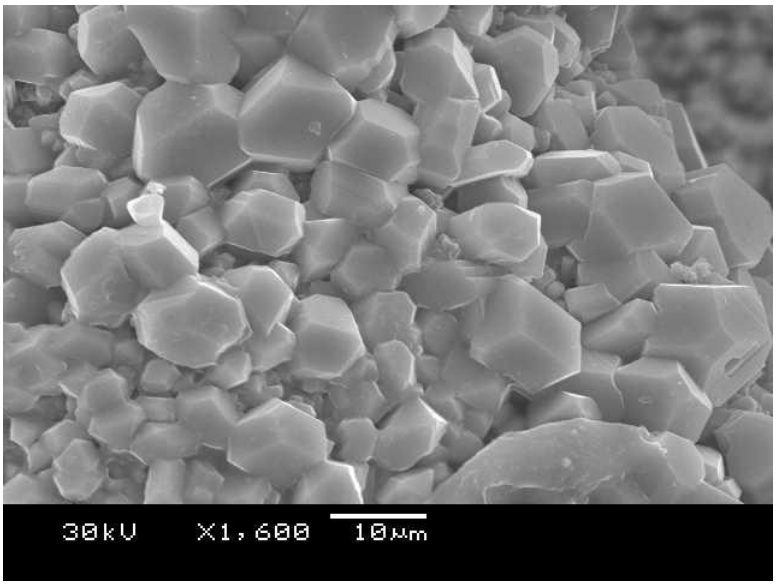

(a)

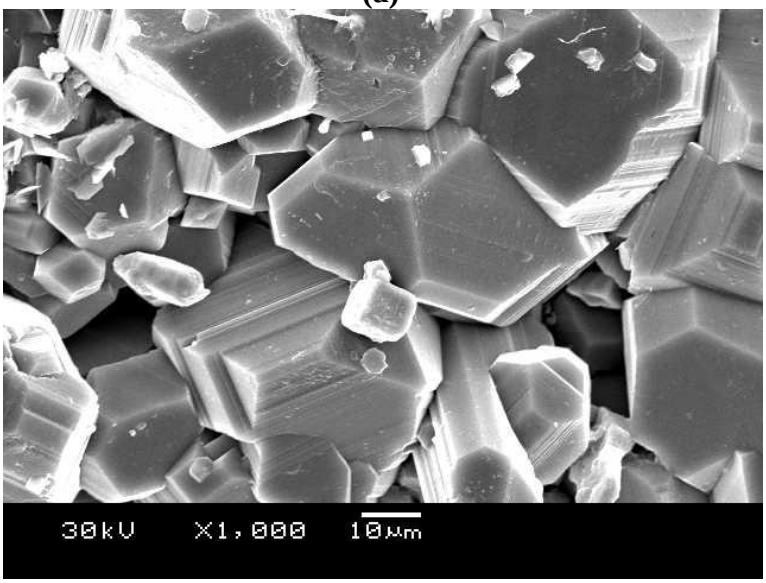

(b)

Figure 3.5 SEM images of the lattice surface after 24 hours of electrochemical reduction; (a) top of the lattice and (b) bottom of the lattice

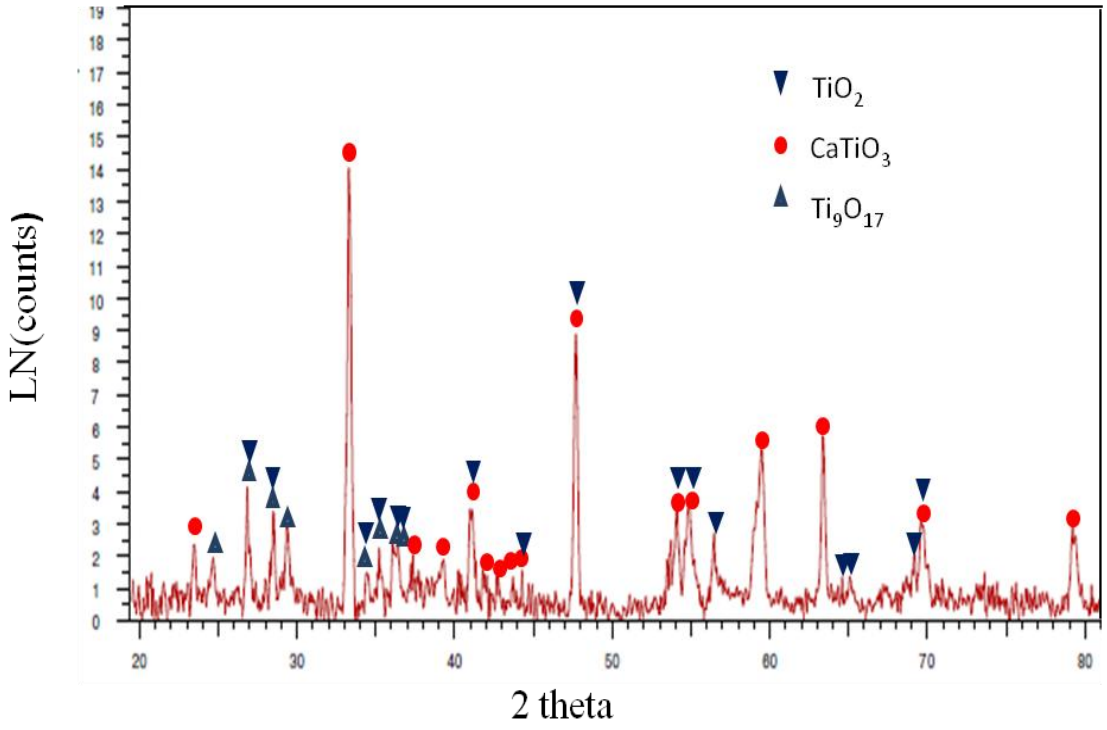

Figure 3.6 XRD pattern after 24 hours reduction of TiO_2 pellet

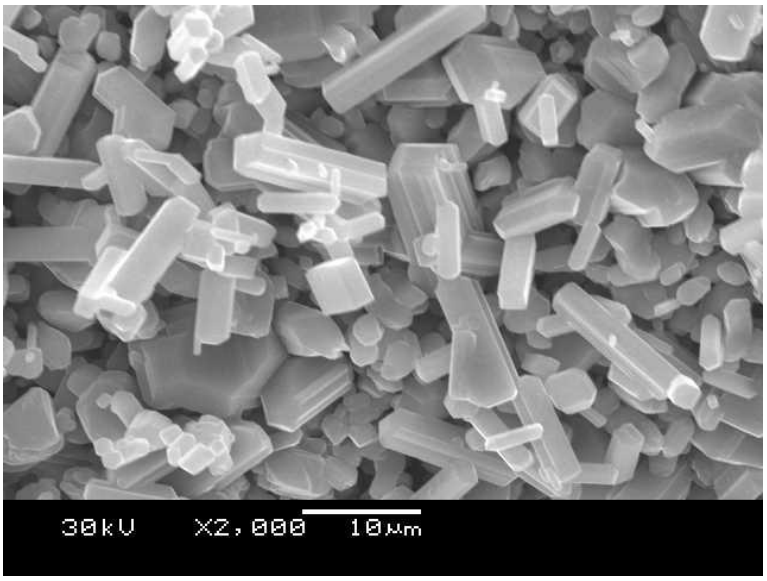

Figure 3.7 SEM image of $CaTi_2O_4$; electrochemical reduction (72hr, 3.2 V, initial current 0.6A)

Figure 3.8 shows the surface of a pellet when current was supplied with a 1.3 ampere and power was initially supplied with 2.5 volts. While the reaction processed, current normally decreased. However, the power was increased upto 4.2 volts to maintain the current at 1.3 ampere. The reduction processe was stopped after 72 hours. About 200 nm fibrous material dominates on the surface of lattice. This fibrous material structure is also analyzed by XRD pattern and it is shown in **Figure 3.9**. TiO, $CaTiO_3$, and titanium sub-oxide was found by pattern analysis. A comparing of XRD pattern and SEM after 24 hr shows that the amount of $CaTiO_3$ was dramatically decreased and TiO ($Ti_{0.93}O$) appeared in the pattern. We also used energy-dispersive X-ray spectroscopy (EDX) to detect the structure of fibrous material and it is shown in **Figure 3.10**. Cacium was marked with a red dot and titanium was marked as a green dot. Large amount of calcium is widely distributed on the surface as shown in **Figure 3.8(a)**. Whereas, calcium did not appeared on the wire shape materials (**Figure 3.8(b)**) but titanium was only detected. Unfortunately the amount of oxigen can not be detected by the EDX which we used in the research. The large particles as shown in **Figure 3.7** are analyzed as $CaTiO_3$, because the red dot and green dot appear togather and we have only $CaTiO_3$ composit from XRD pattern. XRD patterns did not show any titanium metal, thus, the fibrous material cannot be titanium. The fiberous material is simply regarded as TiO because XRD pattern of $Ti_{0.93}O$ appeared after 72 hours of reduction.

The $CaTi_2O_4$ production step was already introduced in the Fray group research. However $CaTi_2O_4$ was not produced and TiO fiber was produced in this experimental condition. Besides the amount of $CaTiO_3$ decreased. It could be suggested that TiO fiber

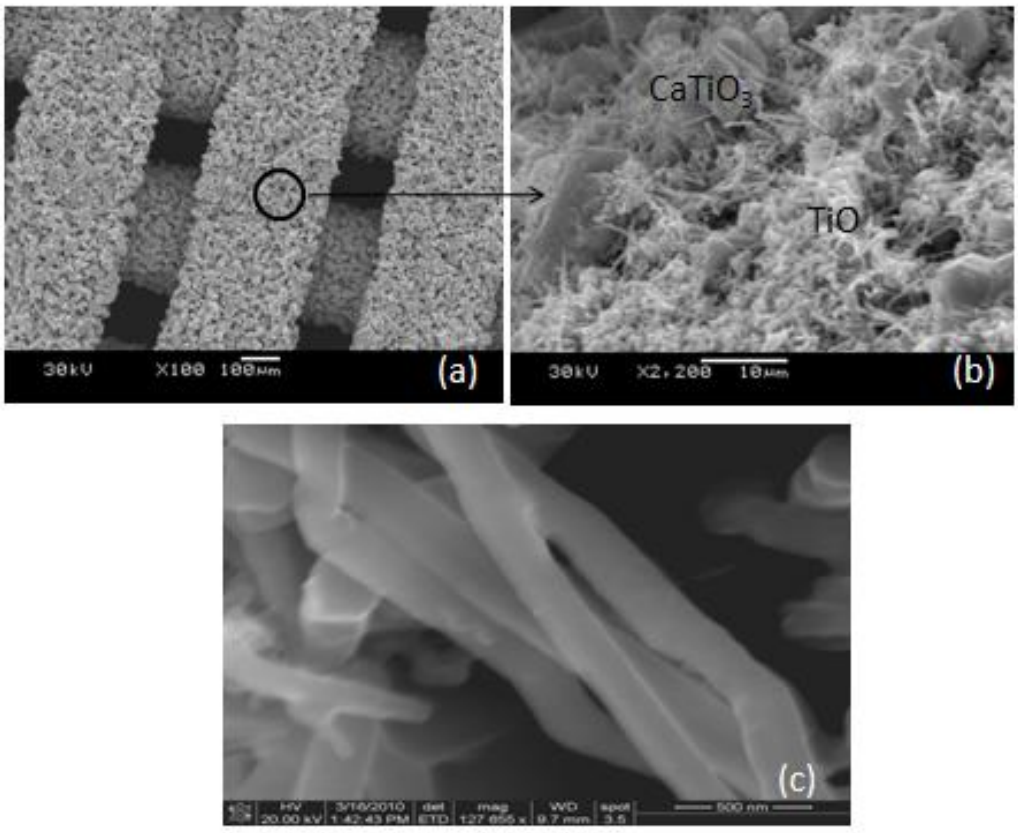

Figure 3.8. SEM of calcium titanite and TiO after 72 hours reduction; (a) lattice surface (b) TiO fiber and calcium titanite on the lattice, (c) TiO fiber

would be produced by consumption of CaTiO3. The hypothesized reaction mechanism on the cathode is :

$$CaTiO_3 + 2e^- = Ca^{2+} + 2O^{2-} + TiO \qquad E^0 = +1383mV \qquad (3.3)$$

where the cell potential at 950˚C is calculated using **HSC** Chemistry 5.1. The reaction producing $CaTi_2O_4$ (equation 1.16) is a redox reaction. This means that the reaction is more favorable than this reaction. The reaction of producing $CaTi_2O_4$ is expected to appear in this step but the reaction does not take place in this stage. It is only produced in

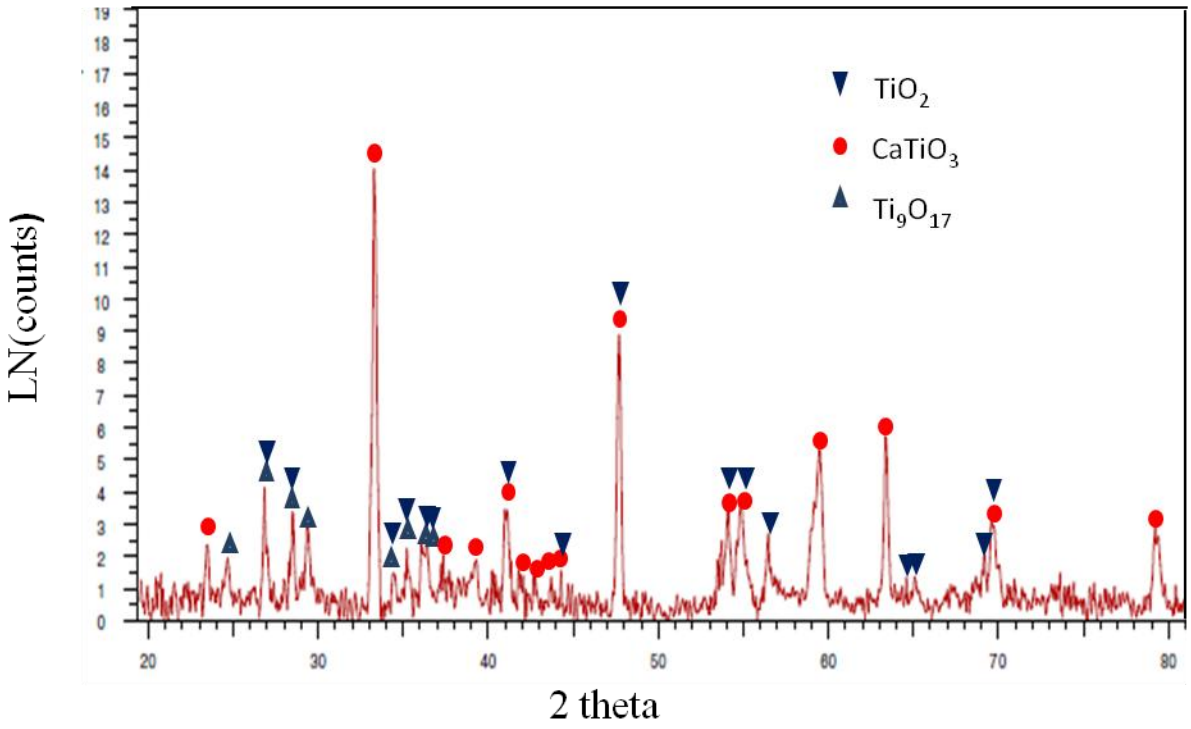

Figure 3.9 XRD pattern after 72 hours reduction of TiO_2 pellet; 4.2 V, 1.3 A at 950 ˚C

the experiments that supply with lower than 3.2 voltage power. It is projected that high voltage conditions produce TiO fiber.

However the reaction stopped at about 74 hours. There are two reasons for this. First, the cromoly wire was rusted by Cl_2 gas which generated in the anode side in a high temperature (950 ^{o}C). Second, $CaCl_2$ was consumed. The consumsion rate of one mole $CaCl_2$ was calculated by cell potential equation with 4.2 voltage (110 g/mol, anhydrous). After the calculation, it takes about 74 hours to consume one mole $CaCl_2$. The graphite crucilbe that used in this reduction process able to contain about 120 g of $CaCl_2$. Thus most $CaCl_2$ was consumed while 72 hours reduction is processed. This create a disconnection between graphit rode and crucible.

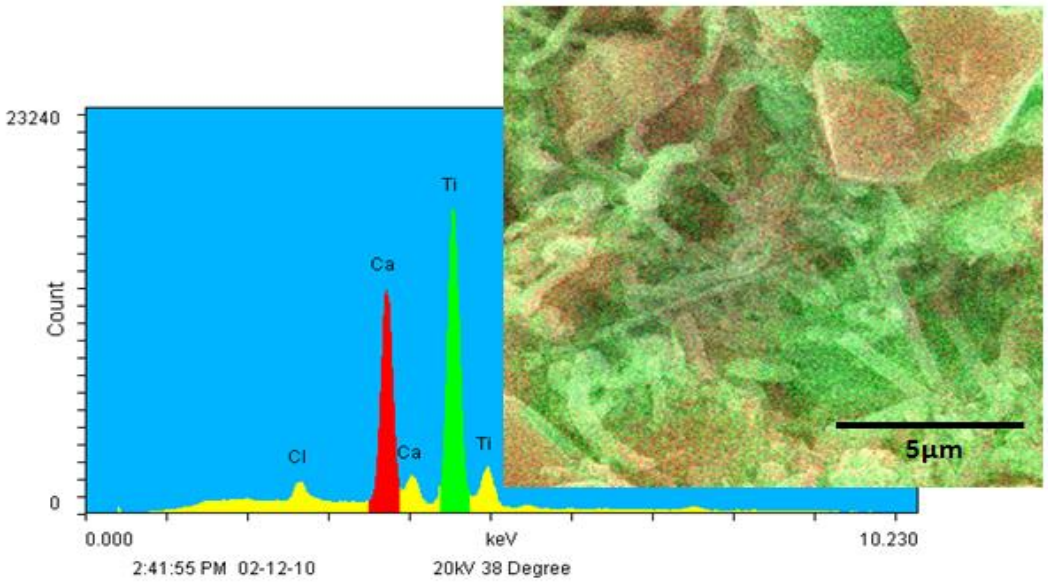

(a)

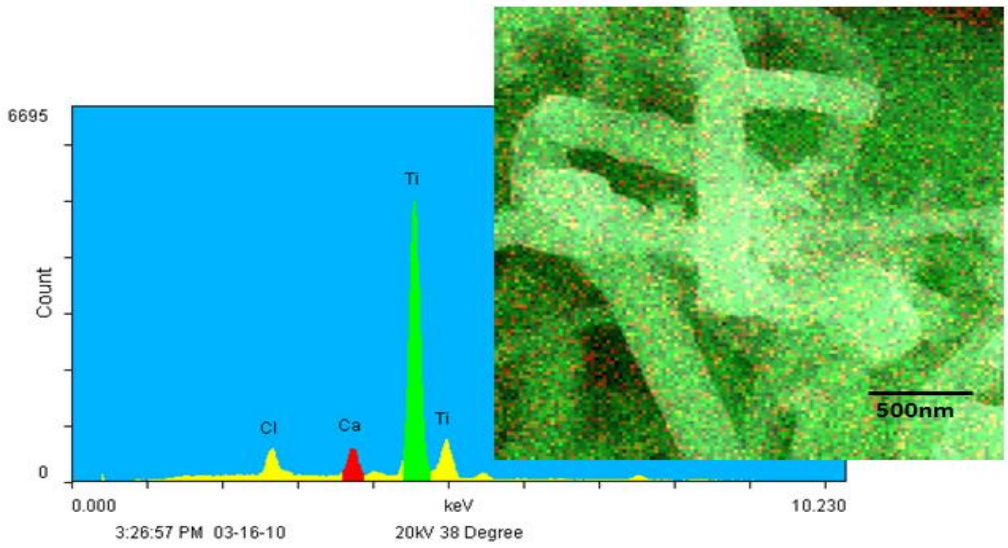

(b)

Figure 3.10 EDS analysis of TiO fiber

CHAPTER 4 CONCLUSION

TiO_2 electrochemical reduction (FFC) was performed in this research. Before the FFC method was carried out, TiO_2 lattices were fabricated by the robocasting method. TiO_2 paste was formulated and characterized using viscosity measurements, which revealed a shear thinning with yield stress rheology suitable for robocasting. The fabricated lattices were lightly sintered an then place into a graphite crucible with molten $CaCl_2$ at 950 ^oC. An electrochemical reaction using a graphite anode and cathod was performed to reduce the TiO_2 structure.

The electrolytic cell was controlled in two different ways. The first case (control) followed the FFC procedure with a 3.2 V potential supplied to the system and maintained until the reduction process stopped. The cell current was observed to decreased during the first 24 hours and then reached a stable state. In the second case (test), cell potential was increased from 2.5 to 4.2 volts during the initial 8 hours of reaction to maintain a steady current flow. The control case produced compositions and particle morphology typically observed in the FFC method (i.e., TiO_x, $CaTiO_3$ and $CaTi_2O_4$). However, titanium metal was not produced in the step due to the limitation of the system to maintain over 72 hours at 950 ^oC. The test condition brought somewhat different results. It produced TiO fiber after 72 hours of reduction.

The test condition process was stopped by several circumstances in about 72 hours. First, the cromoly wire was corroded and broken by Cl_2 gas. Second, the level of the molten $CaCl_2$ electrolyte decreased due to consumption of the electrolyte a the high

voltage condition. Thus, this problem must be solved to continue the process longer. However, this problem can be simply solved by introducing a larger graphite crucible, high resistance metal wire, and fast inert gas flow to the system. To design the accurate crucible, a complete reaction termination time must be studied. If the termination time is not certain, a side chamber should be used containing $CaCl_2$ salt to support it continusely as much as $CaCl_2$ consumed. If the reaction can be processed continuously, TiO fiber is not the only product but Ti fiber or Ti metal can also be produced from the system. Furthermore, TiO fiber is an intermediate product. Thus it usually remained with other type of titanium sub-oxide and calcium titanates. Separation methods for the TiO fiber should be considered in the future studies.

This fibrous TiO material is new and has not yet been reported. The characterization of TiO fiber is not yet reported. Thus it is difficult to predict its application. Studies for TiO properties must be carried in the future. There are some studies of application using intermediate product mainly titanium sub-oxide from FFC methods. [39]

REFERENCES

1. Alper J. Biology and the Inkjets, (2004*) Science* 305:1895
2. Giordano R.A., Wu B.M., Borland S.W., Cima L.G., Sachs E.M., Cima M.J., *Journal of Biomaterials Science*, Polymer Edition. 8(1):63-75, 1996
3. J. E. Grau, S. A. Uhland, J.H Moon, M.J. Cima, E. Sachs, *J of American Ceramic Society* 82(8), (1999)
4. R.K. Holman, S.A Uhland, M.J. Cima, E. Sachs, *J colloid Interface Sci*, 274(2), (2002)
5. R.K. Holman, M.J. Cima, S.A Uhland, E. Sachs *J Colloid and Interface Science*, 249(2), 2002, 432-440
6. Agarwala M.K., Bandyopadhyay A., Weeren R.V., Safari A. Danforth S.C., Langrana N.A., Jamalabad V.R. Whalen P. *J., Ameerican Ceramic Soc Bul*, 75(11), (1996)
7. A. Bandyopadhyay, R.K. Panda,V.F. Janas, M.K. Agarwala, S.C. Danforth, A.Safari, J. Am. Ceram. Soc., 80(6), (1997)
8. J.E. Smay, G.M. Gratson, R.F. Shepherd., J.A. Lewis, *Advanced material*, 14(18), (2002)
9. J.E. Smay, B.A. Tuttle, Cesarno III J., J.A. Lewis, *J Am. Ceram. Soc*., 87(2), (2004)
10. Cesarano, J. I.; Calvert, P. D. Freeforming objects with low-binder slurry. 6027326, 2000.
11. Smay, J. E.; Cesarano, J.; Tuttle, B. A.; Lewis, J. A., Piezoelectric properties of 3-X periodic Pb(ZrxTi1-x)O-3-polymer composites. *Journal of Applied Physics* **2002,** 92, (10), 6119-6127.
12. Smay, J. E.; Cesarano, J.; Lewis, J. A., Colloidal inks for directed assembly of 3-D periodic structures. *Langmuir* **2002,** 18, (14), 5429-5437.

13. Smay, J. E.; Nadkarni, S. S.; Xu, J., Direct writing of dielectric ceramics and base metal electrodes. *International Journal of Applied Ceramic Technology* **2007,** 4, (1), 47-52.
14. Smay, J. E.; Gratson, G. M.; Shepherd, R. F.; Cesarano, J.; Lewis, J. A., Directed colloidal assembly of 3D periodic structures. *Advanced Materials* **2002,** 14, (18), 1279
15. Cesarano, J.; Stuecker, J. N.; Dellinger, J. G.; Jamison, R. D. 'Method for making a bio-compatible scaffold'. 6993406, 2006
16. Michna, S.; Wu, W.; Lewis, J. A., Concentrated hydroxyapatite inks for direct-write assembly of 3-D periodic scaffolds. *Biomaterials* **2005,** 26, (28), 5632-5639.
17. Jian Xu, Design 'Assembly and Characterization of Composite Structures of Barium Titanate and Nickel', Oklahoma State University, (2010)
18. Rueb, C. J.; Zukoski, C. F., Viscoelastic properties of colloidal gels. *Journal of Rheology* **1997,** 41, (2), 197-218.)
19. Ogden, H.R and Gonser, B.W.: 'Titanium', Rare Metals Handbook, Edited by C.A Hampel, Reinhold Press Co., New York 455(1956)
20. Van Arkel, A. and De Boer, J, Z *anorg, chem*., 148, 345(1925)
21. W. J. Kroll, *J. of the Electrochemical Society*, 78, 35 (1940)
22. E.C. Perkins, H. dolezal, D.M. Taylor, R.S. Lang, : 'Fludized-Bed Chlorination of Titaniferrous Slags & Ors', Bureau of Mines RI 6317, (1963)
23. H.M. Harris, A.W. Hederson, T.T. Campbell, *light metals*, 1, 299 (1973)
24. A.R. Chughtai, H.M. Harris, Jr.J.R. Riter, *Metall. Trans*. B. 8B, Sep., 507, (1977)
25. T.A Henrie,: 'extactive Metallurgy of Titanium', High Temperature Refractory Metals Conference, New York, Feb., 1965, TMS-AIME Conference, 34, part 1, 139 (1968)
26. Dooley III G.J., *J of metals*, 8 (1975)
27. Noda Toshia, *J of Metals*, 12 (1988)
28. M.A. Hunter, *J of Americal Chemical Society*, 32, 330 (1910)
29. J.B. Rosenbaum, 'Light metals 1982', edited by J.E. Anderson, Proc, 111th, AIME Annu. Meeting, AIME, New York, 1123 (1981)
30. M.J. Rand, I.J. Reinert, *J. Electrochemical Soc*.., 111, 429 (1954)

31. O. Q. Leone, H. Knudsen, and D. E. Couch, *J. of Metals*, 19(3)(1967)
32. Y. Hashimoto,, K. Uriya, R. Kono, *Denki Kagaku*, 39(6)(1971)
33. Y. Hashimoto, *Denki Kagaku*, 39(12)(1971)
34. Y. Hashimoto,, K. Uriya, R. Kono, *Denki Kagaku*, 40(1)(1972)
35. A.J. Becker, D.R. Careatti , US Air Force Report, AFMLTR-79-4147, Wright-Patterson AFB, Ohio (1979)
36. G.Z. Chen, D.J. Fray, T.W. Farthing, *Nature*, (2000), 361, 407.
37. D.J. Fray, T.W. Farthing, G.Z. Chen, US patant, WO9964638, (2000).
38. C. Schwandt, D.J. Fray. *Electrochemica Acta*, 51, 66, (2005).
39. K. Wang, K. kiang, J.Lu, l. Zhuang, C. Cha, X. Hu, G.Z. Chen, *J. Power Sources*, 185 (2008) 892
40. Massalsky T.B., 'Binary Alloy Phase Diagrams', ASM International Materials Park, OH, (1990)
41. Z. Liu, d.D. Sun, P. Guo, J.O. Leckle. *Nano Letter*, 7, (2007), 1081.
42. J. Zarzyski, *J. Sol-Gel Sci. Tech*., 8 (1997)
43. M.D. Banus, T.B.. Reed, A.J. Strauss, *Physical Review*, B5, (1972), 2775

VITA

Jeongwook Seo

Candidate for the Degree of

Master of Science

Thesis: ELETROCHEMICAL REDUCTION OF TITANIUM DIOXIDE 3-D PERIODIC STRUCTURES

Major Field: Chemical Engineering

Biographical:

Education:

Completed the requirements for the Master of Science in Chemical Engineering at Oklahoma State University, Stillwater, Oklahoma in | December, 2010

Completed the requirements for the Master of Science in Chemical Engineering at Chungbuk National University, CheongJu, Chungbuk, S.Korea, 2004.

Completed the requirements for the Bacheorl of Science in Chemical Engineering at Chungbuk National University, CheongJu, Chungbuk, S.Korea, 2002.

Experience:

Nov. 2005 – Jun. 2007 **Researcher,** Quantum Optics Laboratory, Korea Atomic Energy Research., Daejeon, Korea

Apr. 2005 – Aug. 2005 **Researcher,** Thin Film Material Research Center, Korea Institute of Science Technology (KIST), Seoul, Korea

Nov. 2004 – Apr. 2005 **Researcher,** DaeJoo Electronic Materials CO., LTD, Siheung, Gyenggi, Korea

Mar. 2002 – Nov. 2004 **Researcher,** Korea Institute of Energy Research (KIER), Deajeon, Korea

Name: Jeongwook Seo Date of Degree: December, 2010

Institution: Oklahoma State University Stillwater, Oklahoma

Title of Study: ELETROCHEMICAL REDUCTION OF TITANIUM DIOXIDE 3-D PERIODIC STRUCTURES

Pages in Study: 43 Candidate for the Degree of Master of Science
Major Field: Chemical Engineering
Scope and Method of Study: Electrochemical Reduction Process, Robocasting.Scanning electron microscopy, Energy dispersive X-ray spectroscopy X-ray diffraction

Findings and Conclusions: The electrochemical reduction of TiO_2 was carried out with 3-D periodic structures which were fabricated by the robocasting. After the process was controlled in high voltage condition, the test condition yields an abundance of TiO nanofibers on the surface of the 3-D lattice. The electrolyte consumption is problematic for the notion of scale-up of this process, but the research produced some interesting TiO fibers that may prove worth the unfavorable reaction conditions. For instance, TiO fibers have not been reported in the literature, but may have application as catalysis material.

Abstract: The conversion of rutile (TiO_2) to TiO is carried out using a molten-salt electrochemical process known as the FFC method. A three dimensional structure of TiO_2 is fabricated by robocasting, a process for assembling complex, three-dimensional (3-D) structures by extruding and patterning colloidal gels (pastes) followed by drying and sintering of the particles. A 3-D lattice structure is fabricated using the robocasting method and the lattice structure is used as the feedstock for a molten $CaCl_2$ electrochemical reduction process. The reduction process is carried out using two different conditions. The control condition (the FFC method) uses a constant 3.2 V cell potential and allows current to vary as limited by the sample size and chemical reactions. The test condition is to maintain a constant current by varying the cell potential from 3.2 V to 4.2 V during the course of the electrochemical reaction.

The control condition produces the expected chemical changes observed by others using the FFC method. The test condition yields an abundance of TiO nanofibers on the surface of the 3-D lattice. For both conditions, the reaction is terminated prior to conversion to Ti metal and the intermediate products are analyzed. The test condition consumes the $CaCl_2$ electrolyte. The electrolyte consumption is problematic for the notion of scale-up of this process, but the research produced some interesting TiO fibers that may prove worth the unfavorable reaction conditions. For instance, TiO fibers have not been reported in the literature, but may have application as catalysis material

ADVISER'S APPROVAL Dr. Jim Smay